Role of Thermal Stress in Athermal Waveguide Design Using TiO_2 Waveguides on a Silicon Substrate

J. T. Bovington*, R. Wu, K. T. Cheng, and J. E. Bowers
Department of Electrical & Computer Engineering, University of California Santa Barbara, California, USA
*Corresponding author: jock@ece.ucsb.edu

***Abstract*—Experimental demonstrations of ring resonators with TiO_2 cores are presented and measured with -2.9pm/K resonance shift. Their thermo-stress-optic behavior was found to be important to their function; therefore an inclusive model is presented and simulated numerically.**

(OCIS codes) Keywords: (160.3130) Integrated optics materials; (230.7370) Waveguides

I. Introduction

Thermal stability is a very real, but often overlooked issue in research even though the need for such athermal structures is clear for photonics applications from low-cost communications links in data centers, passive optical networks, microwave photonic filters and sensors, to high performance avionics and other military applications. The current solution is to avoid the issue, by using a single channel, course WDM (~20nm or more channel spacing), localized heaters with temperature stabilizing feedback loops, or for DWDM a power hungry thermo-electric cooler (TEC). Each of the current solutions sacrifices performance or power.

This is an active research area with a number of solutions to address this challenge by designing intrinsically athermal structures. We would classify them into circuit based approaches [1] and materials solutions. Among the materials solutions, the overwhelming majority have been polymers [2]. Oft-quoted issues with these polymer-based solutions include process compatibility, degradation, reliability, and narrowed operating conditions. Much work to address these concerns continues and in the end such solutions may find a home in certain applications. However, titania (TiO_2) has recently been suggested as a CMOS compatible alternative material to polymer for enable athermal waveguides in photonic integrated circuits [3]. The reason for this is its strong negative material thermo-optic coefficient (MTOC) ($1/n \cdot dn/dT$). Literature has shown its MTOC in a range of $-(1\text{-}6.5)\times10^{-4}\ K^{-1}$.

In this paper we present some recent experiments with ring resonators using TiO_2 as a core material rather than a cladding layer as previously demonstrated for athermal designs. As a result this raises some important, under-published issues that are particularly pertinent for TiO_2 based waveguide design; namely, the suppression of MTOC and perhaps an explanation for the large range of literature values for this property.

Our measurements indicate that buried TiO_2 core waveguides clad by plasma assisted vaper depsition SiO_2 with core confinements ranging from 0.07 to 0.42 exhibit waveguide thermo-optic coefficient (WTOC) ($1/n_{eff} \cdot dn_{eff}/dT$) on order of the published SiO_2 MTOC ($\sim10^{-5}K^{-1}$) regardless of confinement. Therefore in some geometries the thermo-stress-optic (TSO) effect can dominate the resulting WTOC, not a MTOC as current literature athermal waveguides using TiO_2 suggests. Finally we apply a theory to explain our results.

II. Waveguide Geometry and Fabrication

A single lithography process with a chromium hard mask was used for all waveguides is outlined in Figure 1. Each core was deposited on 15 microns of thermal oxide to eliminate potential substrate leakage for certain thin core geometries. Amorphous TiO_2 was DC sputtered at 2300W in an Ar/O_2 (20/10sccm) environment with a Ti target at room temperature in an Endeavor tool. The measured index was 2.18 at 1550nm as measured in a J.A. Woollam Co. Inc variable angle spectroscopic ellipsometer (VASE). Si_3N_4 was deposited using low pressure chemical vaper deposition on both sides of the wafer using a stociometric process with a refractive index of 1.98 at 1550nm as measured in the VASE. High density SiO_2 films used as cladding above the core were deposited at 300°C.

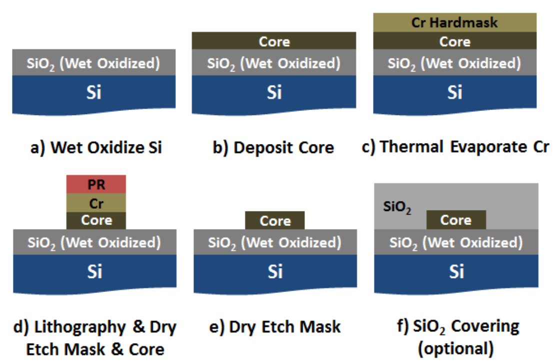

Fig. 1. Generic process flow for all waveguides in this publication.

Lithography was done using an ASML PAS 5500/300 deep ultra violet photolithography tool. Dry etching was done with an inductively coupled plasma etcher for the Cr hardmask with a Cl_2/O_2 chemistry, followed by a $CHF_3/CF_4/O_2$ dry-etch of the core. This core etch sufficiently removed the photo-resist softmask such that only the Cr remained. The Cr was then dry-etched. The revealed core was cleaned with O_2 plasma to

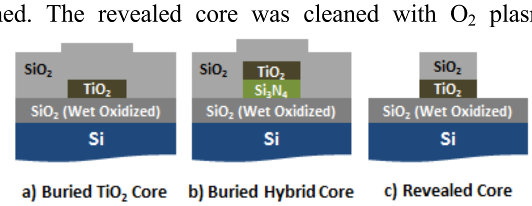

Fig. 2. Cross section of waveguide designs with TiO_2 or hybrid cores.

remove the remaining polymer from the ICP etches. Buried waveguides had additional oxide over cladding. The samples were then diced and tested as described below in Section III.

Figure 2 shows the three waveguide cross sections reported in this work. Of note is the buried versus revealed designs. This was most significant in the resulting thermal drift measured.

III. MEASUREMENT SETUP AND RESULTS

Using a tunable laser, polarization controller, lensed fiber couplers and a photo diode, we tracked the TE resonance of the through port of ring resonators with temperature (15-40°C) for a range of waveguide geometries. These waveguides have a range of material confinement factors simulated in Fimmwave. We were able to demonstrate a suppression of the WTOC to ~$10^{-6}K^{-1}$ by burying it in oxide top cladding. This effect is released when the side wall of the TiO_2 is reveal by co-etching the top cladding/ridge and the core as shown in Figure 2c. The resulting effect is plotted in Figure 3 resulting in resonant shifts as low as -2.9pm/K. Various waveguide widths were used, so the confinement factor is plotted for comparison.

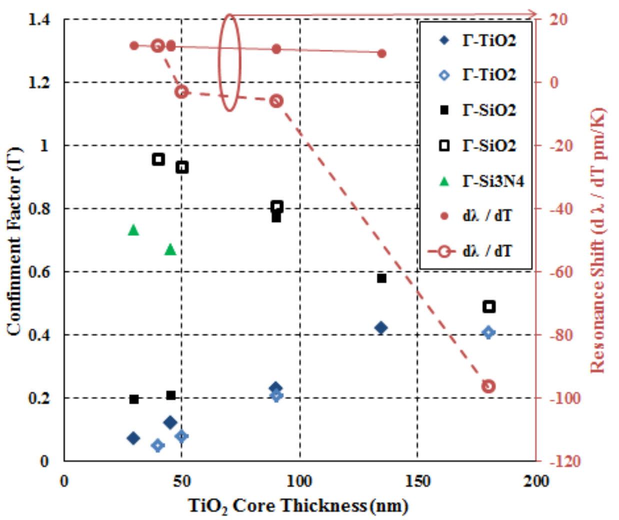

Fig. 3. Ring resonance drift for buried TiO_2 and buried hybrid TiO_2/Si_3N_4 core waveguides (solid points and line). The substantially muted change is thermal drift with confinement factor corresponds to dn/dT of TiO_2 ~-10^{-6}. Hollow points and dotted lines signify revealed structures. Lines mearly guide the eye to the secondary axis in red.

IV. THEORY AND SIMULATION

The relation of index with density can explain these measurements with the addition of TSO terms to the theory used in [3-4]. The resonance shift with temperature can be expressed as [5]:

$$\frac{d\lambda_r}{dT} = \lambda_r \left[\frac{1}{n_{eff}} \frac{dn_{eff}}{dT} + \alpha_{sub} - \frac{1}{E} \frac{d[\nu(\sigma_{xx}+\sigma_{yy})-\sigma_{zz}]}{dT} \right] \quad (1)$$

where

$$\frac{dn_{eff}}{dT} = \frac{\partial n_{eff}}{\partial T} + \frac{\partial n_{eff}}{\partial \sigma_{ii}} \frac{d\sigma_{ii}}{dT} \quad (2)$$

λ_r is the resonant wavelength, α_{sub} is the thermal expansion coefficient of the silicon substrate, E is Young's modulus, ν is Poisson's ratio, σ are the orthogonal stress coefficients, and n_{eff} is the effective index of the mode. The third term within the square bracket of Equation 1 is from the stress induced waveguide path-difference change; the second is the contribution from the thermal expansion of the substrate and is not path length dependent. Finally, the first term in Equation 1 is a result of small index variations in the waveguide. As stated in Equation 2, nested in $\frac{dn_{eff}}{dT}$ is a great deal of physics including TSO effects. 2D COMSOL Finite Element Method simulations were done combining the mechanical stresses with the optical properties to calculate $\frac{d\lambda_r}{dT}$. The details of these simulations will be presented at the conference. The simulation uses a generalized plane strain method to apply mechanical stresses to the layers inputting E, ν, and linear thermal expansion coefficients for all materials including the silicon substrate. Then it assumes TiO_2 and SiO_2 are isotropic and therefore the refractive indices relation with the stress optic coefficients is described by two stress-optic (piezo-optic) coefficients B_1 and B_2 as shown in Equation 3 where n_0 is the index without stress, and $dn_{ii,}$ and σ_{ii} are the stress induced index change and stress coefficient respectively for each orthogonal direction. $dn_{ii,}$and σ_{ii} are functions of temperature T.

$$\begin{bmatrix} dn_{xx}(T) \\ dn_{yy}(T) \\ dn_{zz}(T) \end{bmatrix} = \frac{n_0^{\,3}}{2} \begin{bmatrix} B_1 & B_2 & B_2 \\ B_2 & B_1 & B_2 \\ B_2 & B_2 & B_1 \end{bmatrix} \begin{bmatrix} \sigma_{xx}(T) \\ \sigma_{yy}(T) \\ \sigma_{zz}(T) \end{bmatrix} \quad (3)$$

V. CONCLUSTIONS

TiO_2 is a very important material for future athermal photonic integrated circuits. TSO effects are important to design and performance of TiO_2 core waveguides. In many cases this effect overshadows non-stress related thermo-optic effects of the material and thus must be included to determine the correct TOC of TiO_2. To generally solve the thermal drift problem without polymers or active integration, further stress research into TiO_2 issue is vital to enable integration of this CMOS compatible material into photonic integrated circuits.

The authors acknowledge support from Intel ARO program, and Semiconductor Research Corporation (SRC) for this research.

[1] B. Guha, K. Preston, and M. Lipson, "Athermal silicon microring electro-optic modulator.," *Optics letters*, vol. 37, no. 12, pp. 2253–5, Jun. 2012.

[2] V. Raghunathan, W. Ye, J. Hu, and T. Izuhara, "Athermal operation of Silicon waveguides: spectral, second order and footprint dependencies," *Opt. Express*, vol. 18, pp. 17631–17639, 2010.

[3] P. Alipour and A. Atabaki, "Athermal Performance in Titania-Clad Microring Resonators on SOI," *... Research, Silicon and ...*, no. 2010, p. IMC6, 2010.

[4] F. Qiu, A. M. Spring, F. Yu, and S. Yokoyama, "Complementary metal–oxide–semiconductor compatible athermal silicon nitride/titanium dioxide hybrid micro-ring resonators," *Applied Physics Letters*, vol. 102, no. 5, p. 051106, Feb. 2013.

[5] M. Huang and X. Yan, "Thermal-stress effects on the temperature sensitivity of optical waveguides," *JOSA B*, vol. 20, no. 6, pp. 1326–1333, 2003.